always measurable. For a given rhenium radical, reaction with MA ($E^{1/2}$ = -0.84 V vs. SCE[30]) is slightly faster than that with MCP^+ ($E_{1/2}$ = -0.66V vs. SCE[5]). The relative rates are in the opposite sense from what we expect, namely that the rate will be faster for the more exergonic process.[27,31] However, it is difficult to make meaningful comparisons of the results, because the two series of reactions were studied in different solvents and involve different charge types.[32]

17-Electron vs. 19-Electron Radicals? The metal carbonyl radicals studied to date have been found to undergo associative ligand substitutions, giving rise to 19-electron intermediates or transition states.[3] Whether 17-electron or 19-electron species are responsible for electron transfer is less clear. In the absence of evidence to the contrary, it has been assumed that 17-electron radicals are capable of acting as reducing agents.[4a,5-7] On the other hand, Tyler and co-workers have favored reduction by 19-electron species in the photochemical disproportionations of dinuclear carbonyl compounds with Lewis bases.[8,33] A Lewis base substituted radical, being more electron-rich than its 17-electron counterpart, should be the more powerful reducing agent, but the question of whether such 19-electron species are kinetically significant remains to be answered. There have been no direct observations of 19-electron radical intermediates by transient techniques, and the kinetic evidence for their existence does not discriminate between a 19-electron transition state or intermediate. It is then questionable whether the equilibrium $ML_n^{\bullet} + L' \rightleftharpoons ML_nL'^{\bullet}$ favors the 19-electron species enough to make its bimolecular electron transfer reactions competitive with those of the 17-electron radical.

Our results suggest that 17-electron radicals undergo rapid electron-transfer reactions. Reaction of $Re(CO)_4L^{\bullet}$ with MA in toluene solution is rapid. There is no possibility of the Re radical reacting initially with a basic solvent molecule, although it might be argued that the base is MA itself; i.e., the reaction may have some inner-sphere character as discussed above. In any case, addition of MA to a rhenium-centered radical is unlikely to enhance the reducing capability of the radical since MA is expected to be a weak nucleophile as a σ-base and is thought to be a stronger π acid ligand than CO.[23a,b] Second, reaction of $Re(CO)_4(P(O\text{-}i\text{-}Pr)_3)^{\bullet}$ with MA exhibits small solvent effects; the rate in toluene (k_T = 1.1 × 10^8 M^{-1} s^{-1}) is marginally less than that in the Lewis base solvents CH_3CN (k_T = 1.9 × 10^8 M^{-1} s^{-1}) and pyridine (k_T = 1.4 × 10^8 M^{-1} s^{-1}). If association to form a 19-electron species occurred to enhance the rate of electron transfer, a much faster rate should be observed in the more nucleophilic solvents. Finally, k_T was determined for the reaction of $Re(CO)_4(PMe_3)^{\bullet}$ with a constant concentration of $MCP^+BF_4^-$ in the presence of varying quantities of added $P(C_6H_5)_3$ in CH_3CN solution. The added phosphine had no effect on k_T at concentrations of up to 0.05 M. The experiment, while interesting, is not conclusive in ruling out a 19-electron intermediate in other cases. Unfortunately, use of a more nucleophilic phosphine is precluded by a direct reaction of phosphine with MCP^+.

Acknowledgment. We are grateful to James A. Wehmer for assistance with the laser flash experiments.

(30) Peover, M. E. *Trans. Faraday Soc.* **1962**, *58*, 2370.
(31) Rehm, D.; Weller, A. *Isr. J. Chem.* **1970**, *8*, 259.
(32) Blandamer, M. J.; Burgess, J. *Coord. Chem. Rev.* **1980**, *31*, 93.
(33) (a) Stiegman, A. E.; Tyler, D. R. *J. Am. Chem. Soc.* **1985**, *107*, 967. (b) Stiegman, A. E.; Tyler, D. R. *Inorg. Chem.* **1984**, *23*, 527.

Structural-Electronic Relationships in Inorganic Solids: Powder Neutron Diffraction Studies of the Rutile and Anatase Polymorphs of Titanium Dioxide at 15 and 295 K

Jeremy K. Burdett,*[†,§] Timothy Hughbanks,[†] Gordon J. Miller,[†] James W. Richardson, Jr.,[‡,⊥] and Joseph V. Smith[‡,§]

Contribution from the Departments of Chemistry and Geophysical Sciences and The Materials Research Laboratory, The University of Chicago, Chicago, Illinois 60637, and The Intense Pulsed Neutron Source, The Argonne National Laboratory, Argonne, Illinois, 60439.
Received July 8, 1986

Abstract: Rietveld analysis of time-of-flight pulsed neutron diffraction of powders shows a nearly isotropic shrinkage of the structures of both the rutile and anatase polymorphs of TiO_2 upon cooling from 295 to 15 K and no change in the sense of the distortion of the TiO_6 octahedra (two long and four short Ti-O distances in both): rutile at 295 (first) and 15 K (second), a_0 4.593 08 (4), 4.586 66 (4), c_0, 2.958 89 (3), 2.954 07 (3), x_{oxygen}, 0.304 76 (6), 0.304 69 (6), Ti-O(4×), 1.9486 (3), 1.9459 (3), Ti-O(2×), 1.9796 (4), 1.9764 (4); anatase at 295 and 15 K, a_0, 3.784 79 (3), 3.782 16 (3), c_0, 9.502 26 (12), 0.504 65 (12), x_{oxygen}, 0.166 86 (5), 0.166 75 (4), Ti-O(4×), 1.9338 (1), 1.9322 (1), Ti-O(2×), 1.9799 (5), 1.9788 (4): all distances (Å) referenced to silicon (a = 5.430 88 Å). Both tight-binding calculations on the crystalline solids and molecular mechanics computations on the oxide lattice alone lead to a model in which the balance of attractive Ti-O and repulsive O-O interactions control the details of the overall structures. The relative bond lengths around metal centers in some other systems are predicted.

Rutile and anatase are two polymorphs of TiO_2 based on distorted close-packed, or eutactic,[1] anion arrays. Accurate crystallographic data have been obtained by powder[2-4] and single-crystal[5-8] X-ray diffraction and single-crystal[9] and powder[10] neutron diffraction; some were obtained at elevated temperatures.[7,8] It is still not clear how the details of the solid-state structure are controlled by the electronic properties of Ti and

[†] Department of Chemistry, The University of Chicago, Chicago, IL 60637.
[‡] Department of Geophysical Sciences, The University of Chicago, Chicago, IL 60637.
[§] The Materials Research Laboratory, The University of Chicago, Chicago, IL 60637.
[⊥] The Intense Pulsed Neutron Source, The Argonne National Laboratory, Argonne, IL 60439.

(1) O'Keeffe, M. *Acta Crystallogr., Sect. A: Cryst. Phys., Diffr., Theor. Gen. Crystallogr.* **1977**, *A33*, 924.
(2) Cromer, D. T.; Herrington, K. *J. Am. Chem. Soc.* **1955**, *77*, 4708.
(3) Nodod, G. *Hamb. Beitr. Angew. Mineral. Kristallphys. Petrog.* **1956**, *1*, 239.
(4) Straumanis, M. E.; Ejima, T.; James, W. J. *Acta Crystallogr.* **1961**, *14*, 493.
(5) Shintani, H.; Sato, S.; Saito, Y. *Acta Crystallogr., Sect. B: Struct. Crystallogr. Cryst. Chem.* **1975**, *B31*, 1981.
(6) Abrahams, S. C.; Bernstein, J. L. *J. Chem. Phys.* **1971**, *55*, 3206.
(7) Meagher, E. P.; Lager, G. A. *Can. Mineral.* **1979**, *17*, 77.

0002-7863/87/1509-3639$01.50/0

Table I. Neutron Powder Diffraction Data and Structure Refinement for Rutile and Anatase

	rutile		anatase	
temp, K	295	15	295	15
space group	$P4_2/mnm$	$P4_2/mnm$	$I4_1/amd$	$I4_1/amd$
a_o, Å neutron	4.593 08 (4)	4.586 66 (4)	3.784 79 (3)	3.782 16 (3)
X-ray	4.593 53 (10)		3.784 79 (7)	
c_o, Å neutron	2.958 89 (3)	2.954 07 (3)	9.512 37 (12)	9.502 26 (12)
X-ray	2.958 75 (3)		9.511 92 (26)	
Z	2	2	4	4
ρ_{calcd} g cm^{-3}	4.250	4.269	3.894	3.905
d_{min}, Å	0.343	0.343	0.351	0.351
d_{max}, Å	3.247	3.247	3.518	3.515
no. of reflctns used	473	473	476	476
no. of parameters	21	21	18	18
R_{F^2}, %	3.38	3.20	3.67	3.08
R_p, %	2.17	2.50	2.06	2.37
R_{wp}, %	3.43	3.88	3.24	3.62
R_{exp}, %	1.66	1.80	2.01	1.94

O.[11-13] Hence we have carried out an accurate redetermination of the structures of these two species at ambient temperature, and the first low-temperature (15 K) determinations, by using the intense pulsed neutron source (IPNS) at the Argonne National Laboratory. This is part of a larger program designed to determine accurately the structures of solids which, although often simple, form the foundation for descriptions of chemical bonding in solids. The structures of many of these were determined at room temperature several decades ago, but with a precision inappropriate for testing out details of modern theory. The newer studies are performed by using powder neutron diffraction for simple phases and single-crystal neutron work for more complex ones. The results of the low-temperature studies ($\sim$10 K) will provide data with which to compare theoretical computations, invariably performed on rigid arrays with no zero-point or other thermal motion. The importance of using low temperature in such studies was underscored by our recent studies of silica polymorphs, for which there are much larger changes from room temperature to $\sim$10 K for the open structure of cristobalite[14] than for the close-packed structure of coesite.[15] Furthermore, the systematic distortion of bond lengths from the "swinging arm" effect is smaller at lower temperature. Studies over a range of temperatures of the changes in the inequivalent distances in the solid will eventually be compared with the anharmonicity in the bond stretching potential. The temperature dependence of the thermal parameters is often useful in exploring how the solid holds together, as we show here. In addition, we will discuss different theoretical ways to regard the geometries adopted by these systems and describe a way to view them.

Experimental Section

Anatase, as supplied by Matheson as titanium dioxide, was checked by powder X-ray diffraction. Rutile was synthesized by heating anatase at 1123 ± 40 K in air for 12 h. This treatment should ensure stoichiometric material.[4] The samples were scaled in cylindrical vanadium cans ($^3/_{16}$ in. diameter, 2 $^1/_4$ in. in length, 0.5-mm wall thickness) in a helium atmosphere and cooled by a two-stage closed-cycle Displex refrigerator. Data were taken on the special environment powder diffractometer at IPNS at controlled temperatures of 295 and 15 K for both samples. Diffraction data from the ±150 °C banks of detectors were fit by using the Rietveld method[16] modified for time-of-flight neutron powder diffraction data.[17,18] Backgrounds were fit with a six-parameter analytical function.[19] Of the seven refinable parameters in the resolution function defining the peak shapes, only those for the Gaussian component related to particle size were refined for anatase. For rutile, an additional refinement of the lagging exponential terms was needed. Pertinent data relating to data collection and structural refinement are presented in Table I. The fit of the experimental data is shown in Figure 1. A small anatase impurity in the rutile sample is not significant for data refinement. Since the material was of high crystallinity, no corrections[20] for the presence of amorphous material were made. Geometrical data for the four studies are given in Tables II–IV.

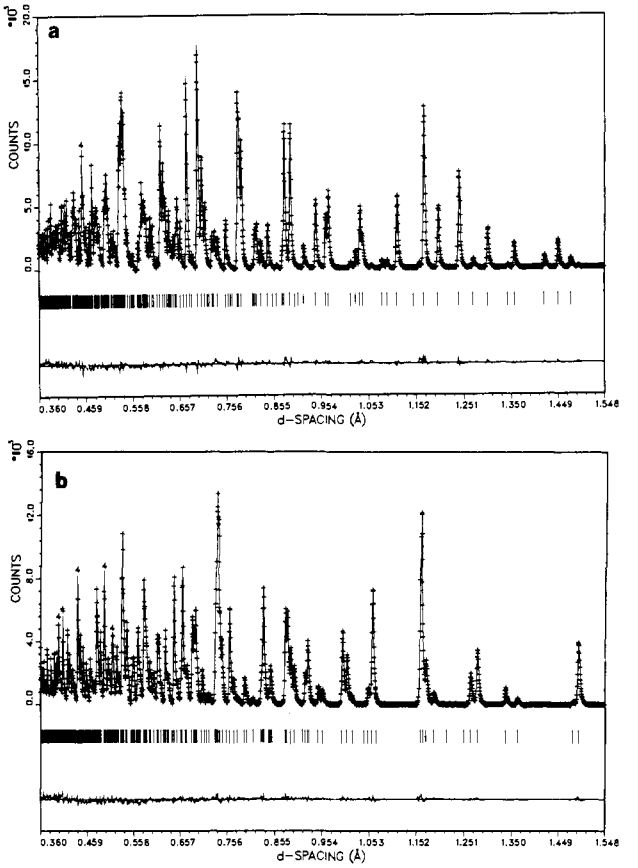

Figure 1. Neutron powder patterns of rutile (a) and anatase (b) at 15 K for d = 0.36–1.55 Å. The difference between the observed data (+) and the calculated profile is shown by the lower profile. All allowed reflections are shown by vertical bars.

(8) Horn, M.; Schwerdtfeger, C. F.; Meagher, E. P. *Z. Krist.* **1972**, *136*, 273.
(9) Gonschorek, W.; Field, R. *Z. Krist.* **1982**, *161*, 1.
(10) Sabine, T. M.; Howard, C. J. *Acta Crystallogr., B: Struct. Crystallogr. Cryst. Chem.* **1982**, *B38*, 701.
(11) Burdett, J. K. *Inorg. Chem.* **1985**, *24*, 2244.
(12) Baur, W. H. *Acta Crystallogr.* **1956**, *9*, 515; **1961**, *14*, 214.
(13) Baur, W. H.; Khan, A. A. *Acta Crystallogr., Sect. B: Structu. Crystallogr. Cryst. Chem.* **1971**, *B27*, 2133.
(14) Smith, J. V.; Pluth, J. J.; Faber, J. *J. Appl. Phys.* **1985**, *57*, 1045.
(15) Smyth, J. R.; Smith, J. V.; Artioli, G.; Kvick, Å. *J. Phys. Chem.* **1987**, *91*, 988.
(16) Rietveld, H. M. *J. Appl. Crystallogr.* **1969**, *2*, 65.
(17) Jorgensen, J. D.; Rotella, F. J. *J. Appl. Crystallogr.* **1982**, *15*, 27.
(18) Von Dreele, R. B.; Jorgensen, J. D.; Windsor, C. G. *J. Appl. Cryst.* **1982**, *15*, 587.
(19) Von Dreele, R. B.; Rotella, F. J., unpublished results.
(20) Richardson, J. W., Jr.; Pluth, J. J.; Smith, J. V. *Acta Crystallogr.*, submitted for publication.

Table II. Atomic Positions and Anisotropic Displacements ($\times 10^3$) of Rutile and Anatase[a]

(a) Rutile

		295 K	15 K
Ti	$x = y = z$	0	0
	$U_{11} = U_{22}$	5.5 (2)	1.2 (2)
	U_{33}	4.5 (3)	1.1 (2)
	U_{12}	−0.3 (3)	−0.2 (2)
	$U_{13} = U_{23}$	0	0
O	$x = y$	0.304 76 (6)	0.304 69 (6)
	z	0	0
	$U_{11} = U_{22}$	5.7 (1)	3.1 (1)
	U_{33}	4.4 (1)	2.6 (1)
	U_{12}	−1.9 (1)	−0.9 (1)
	$U_{13} = U_{23}$	0	0

(b) Anatase

		295 K	15 K
Ti	$0, {}^1/_4, z$	0.375	0.375
	$U_{11} = U_{22} = U_{33}$	3.8 (2)	0.9 (1)
	$U_{12} = U_{13} = U_{23}$	0	0
O	$0, {}^1/_4, z$	0.166 86 (5)	0.166 75 (4)
	U_{11}	4.3 (2)	2.3 (1)
	U_{22}	11.0 (3)	4.8 (2)
	U_{33}	5.8 (1)	3.3 (1)
	$U_{12} = U_{13} = U_{23}$	0	0

[a] The general form for the temperature factor is $\exp[-2\pi^2(U_{11}h^2a^{*2} + \ldots + 2U_{23}klb^*c^*)]$.

To check the cell dimensions obtained from the IPNS-SEPD, X-ray powder patterns at room temperature were obtained for mixtures of rutile or anatase with pure silicon powder (a = 5.430 88 Å) mounted on a digitally-controlled Norelco diffractometer. On average, the four cell dimensions for rutile and anatase (least-squares fits of 17 and 25 reflections from 68 to 144° (2θ); Cu Kα) were 0.025% lower for the X-ray than the neutron determinations. It was presumed that the calibration of the IPNS-SEPD needed modification, and the observed cell dimensions were multiplied by 0.997 48 to give the values in Table I. The revised values for rutile are consistent within 2σ error limits with those given in ref 6 and 7.

The Structures

Rutile may be described as a tetragonal variant of the orthorhombic $CaCl_2$ structure. This arrangement (Figure 2) is one of the possible ways of filling half of the octahedral holes of a hexagonal close-packed array of oxide ions to give a system with the MO_2 stoichiometry. Chains of edge-sharing octahedra, linked to each other by sharing vertices, are a striking feature of this structure. In the $CaCl_2$ structure the oxide ions are coordinated by three metal atoms in a distorted trigonal-pyramidal geometry, point symmetry C_s. The $CaCl_2$ to rutile transformation leads to a structure where these pyramids have become rigorously planar (point symmetry C_{2v}) with a unique O–Ti–O angle of about 99°. The metal octahedra are not regular, and four short and two long Ti–O distances are found, irrespective of the temperature of the structure determination.

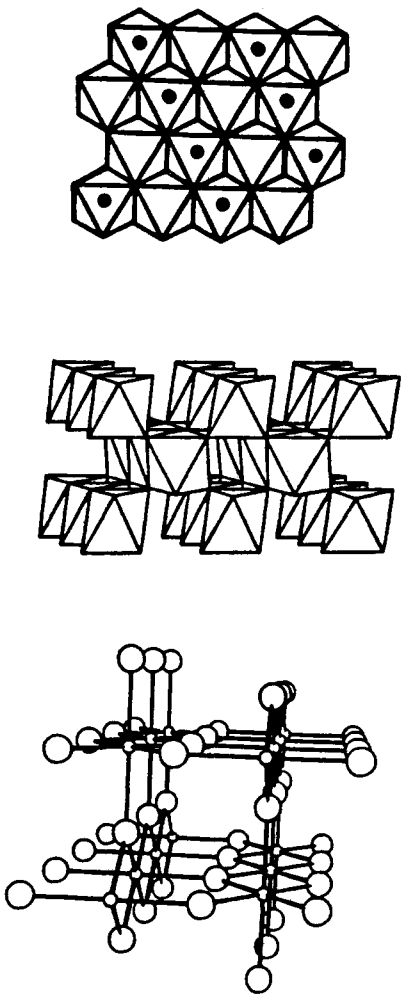

Figure 2. Some views of the rutile structure. The occupation of the octahedral holes in the close packed array, and a polyhedral and ball-and-spoke model are shown (oxygen atoms, large circles).

The anatase structure may be analogously derived from a cubic close-packed array of oxides ions. The sense of the distortion around the Ti atom is similar to that for rutile and is maintained

Table III. Interatomic Distances (Å) and Angles (deg) for Rutile and Anatase

		rutile		anatase	
		295 K	15 K	295 K	15 K
Ti–O	4x	1.9486 (3)	1.9459 (3)	1.9338 (1)	1.9322 (1)
Ti–O′	2x	1.9796 (4)	1.9764 (4)	1.9799 (5)	1.9788 (4)
O–Ti–O	2x	98.79 (2)	98.76 (2)	92.43 (1)	92.42 (1)
O–Ti–O	2x	81.21 (2)	81.24 (2)	92.43 (1)	92.42 (1)
O–Ti–O	2x	180.00	180.00	156.23 (3)	156.30 (2)
O–Ti–O′	4x	90.00	90.00	78.12 (1)	78.15 (1)
O–Ti–O′	4x	90.00	90.00	101.88 (1)	101.85 (1)
O′–Ti–O′	1x	180.00	180.00	180.00	180.00
Ti–O–Ti	2x	130.60 (1)	130.62 (1)	101.88 (1)	101.85 (1)
Ti–O–Ti	1x	98.79 (2)	98.76 (2)	156.23 (3)	156.30 (2)

Table IV. Oxygen–Oxygen Distances (Å) in Rutile and Anatase[a]

rutile			anatase		
295 K	15 K	diff	295 K	15 K	diff
2.7778 (1)	2.7736 (1)	0.0042 (2)	2.4664 (6)	2.4656 (5)	0.0008 (11)
2.9788 (1)	2.9541 (1)	0.0047 (2)	3.0391 (1)	3.0363 (1)	0.0028 (2)
2.5364 (8)	2.5338 (8)	0.0026 (16)	2.7922 (3)	2.7896 (2)	0.0026 (5)

[a] The shared edges are the shortest ones in each case.

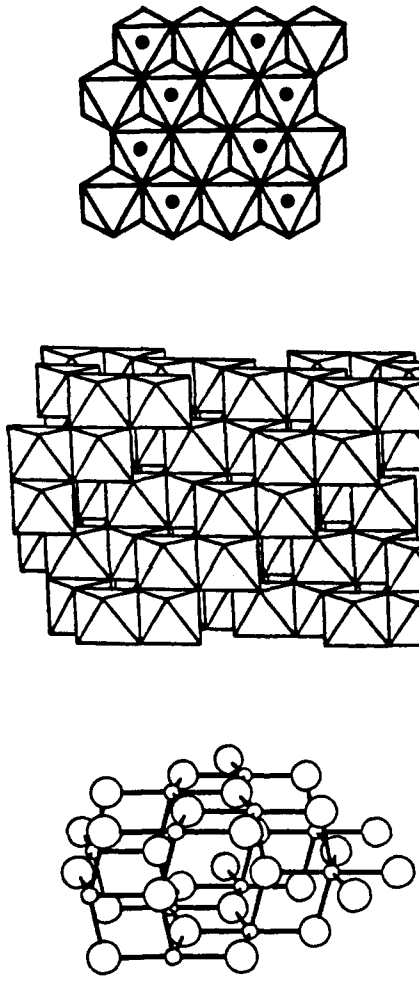

Figure 3. Some views of the anatase structure. The occupation of the octahedral holes in the close packed array, and a polyhedral and ball-and-spoke model are shown (oxygen atoms, large circles).

at low temperature, although the temperature sensitivity appears to be a little less. The TiO_6 octahedron in anatase shares four edges compared to the two in rutile. As a result of such sharing, there are short O–O distances in both polymorphs Table IV. In anatase the shortest is ~0.1 Å shorter than in rutile. Figure 3 shows some views of the structure.

Thermal Expansion

The cell dimensions obtained by neutron diffraction should provide accurate values of the mean thermal expansion (α) from 15 to 295 K (rutile, a, 5.0 (1) × 10^{-6}, c, 5.8 (2) × 10^{-6}; anatase, a, 2.5 (1) × 10^{-6}, c, 3.6 (1) × 10^{-6}). The values of the anisotropy (α_c/α_a) are greater than unity (rutile, 1.16 (6); anatase 1.4 (1)) but smaller than those obtained near 300 K by dilatometry and X-ray diffraction (rutile, 1.30, 1.25, 1.43, 1.25; anatase, 1.74, 2.1).[21] This is consistent with the increase of anisotropy found with temperature increasing from 323 to 963 K[21] and indicates that the anisotropy increases monotonically from 15 to ~1000 K. The values of the thermal expansion from 15 to 295 K are smaller than those near 320 K (rutile, a, (6.1–7.2) × 10^{-6}, c, (7.6–9.9) × 10^{-6}; anatase, a, 3.8 and 4.7 × 10^{-6}, c, 7.8 and 8.2 × 10^{-6}),[21] again in accord with a monotonic increase with temperature.

The greater thermal expansion along c than along a can be related phenomenologically to the observed fractional changes in the O–O distances (Table IV). If the rutile and anatase structures are regarded as frameworks built from oxygen–oxygen struts (see next section), the smaller expansion of the shared O–O edges than of the unshared ones produces the observed anisotropy (cf. ref 21 for a qualitative use of the O–O distances).

Atomic Displacements

Because there is no evidence for a phase transition, it is assumed that the ellipsoidal approximation to the temperature factor (U_{ij}, Table II) represents the thermal motion about a single center-of-motion for each atom. The smaller values of U_{33} (parallel to c) than for the U_{11} and U_{22} of both Ti and O in rutile are indicative of a greater tendency for the atoms to vibrate perpendicular rather than parallel to the edge-shared octahedral chains. Furthermore, the negative value of U_{12} for oxygen indicates that this atom tends to vibrate in the 45° direction [110] out of the plane of the three O–Ti bonds. In anatase the maximum displacement of the oxygen is out of the plane of the O–Ti bonds[8] in a very pronounced way. The somewhat lower temperature sensitivity of the Ti–O distances in anatase may then well be due to this large motion of the oxygen atom perpendicular to the plane containing the three titanium atoms bound to it.

At 15 K, the atomic displacements are responding mainly to the zero-point energy, and the smaller displacements for Ti than for oxygen in both rutile and anatase seem plausible for a simple vibration model in which a heavier Ti atom vibrates less than a lighter O atom (cf. data for Si and O in many framework structures, e.g., ref 22 and 23). However the relative temperature sensitivity of the thermal motions of Ti and O in both rutile and anatase is unusual. Whereas the displacement of a heavier cation is considerably less than that of a lighter anion at all temperatures in most structures, including the rutile-like species MgF_2 and MnF_2,[13] it is not so for rutile at room temperature (Table II), as already noted by Gonschorev and Feld.[9] In both rutile and anatase, the U values for Ti increase over twice as much on average as for O as the temperature increases from 15 to 295 K. In rutile, this increase results in comparable values for Ti and O at 295 K, whereas in anatase the U values for O remain greater than for Ti from room temperature to 1073 K.[8] We will outline an explanation for these results below.

Results and Band Structure Calculations

In an earlier theoretical study[11] we examined an idea by O'Keeffe[1] that the gross structure adopted by "ionic solids" was the one of maximum volume subject to a constant anion–cation distance. Indeed, with this restriction, the geometry of the set of anions alone at the arrangement of minimum energy computed via a tight-binding calculation is close to that observed for the oxide ions in real rutile TiO_2. In orbital terms it is then the closed-shell repulsions of the oxide lattice which determine the structure. (O'Keeffe stressed the importance of ionic interactions between the anions, but the general idea is similar.) We found[11] another effect associated with the oxide ion in the structure. The planar geometry at oxygen is stabilized by π-back-donation associated with overlap of a metal d orbital with the oxygen p orbital which lies perpendicular to the Ti_3 plane defined by each planar OTi_3 unit. Several analogous examples exist in molecular chemistry.[24] Similar effects occur in the structure of crystalline NbO.[25]

Computations of the extended Hückel type[26] which we use as a basis for the tight-binding solid-state calculations[27] are in general not very good for the estimation of equilibrium bond distances, but an extensively used technique does give clues to the relative bond lengths in compounds. A population analysis of the occupied orbitals resulting from a calculation in which all the symmetry-inequivalent distances were set equal very often indicates which will be shorter and longer in the real system. Here then arises a problem, shown in **1** for rutile. The results of the population analysis from our earlier study predict the opposite sense of the distortion around the octahedron to that actually observed. As we also pointed out, the relative sizes of the populations are

(21) Rao, K. V. K.; Naidu, S. V. N.; Iyengar, L. *J. Am. Ceram. Soc.* **1970**, *53*, 124.

(22) Kvick, Å.; Stah, K.; Smith, J. V. *Z. Kristallogr.* **1985**, *171*, 141.
(23) Smith, J. V.; Artioli, G.; Kvick, Å. *Am. Mineral.* **1986**, *71*, 727.
(24) Albright, T. A.; Burdett, J. K.; Whangbo, M.-M. *Orbital Interactions in Chemistry*; Wiley: New York, 1985.
(25) Burdett, J. K.; Hughbanks, T. *J. Am. Chem. Soc.* **1984**, *106*, 3101.
(26) Hoffmann, R. *J. Chem. Phys.* **1963**, *39*, 1397.
(27) For connections between the energy levels of molecules and solids see, for example: Burdett, J. K. *Prog. Solid State Chem.* **1984**, *15*, 173.

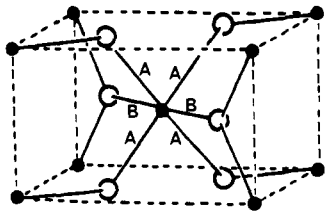

1

however in accord with those we found in distorting an OTi_3 unit away from the trigonal-planar geometry. **2** shows the usual

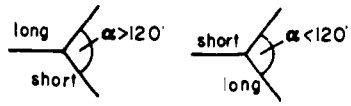

2

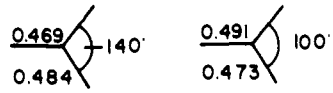

3

dependence of bond length on angle in molecules, and **3** shows the computed overlap populations for an OTi_3^{10+} fragment in the rutile structure **1**. Because the sense of the computed overlap populations in rutile TiO_2 is the same as that found in our computations[11] on stishovite (SiO_2 in the rutile arrangement), the results are not apparently due to special properties of the transition metal.

The atomic arrangement in anatase leads to a less thermodynamically favored polymorph relative to rutile, and our earlier study suggested that half of the energy difference came from an unfavorable anion packing and the rest from a less favorable local anion coordination environment. Here the anion coordination is planar too, but the structure is approximately T-shaped with a unique angle of about 156°. So the distortion at the oxygen away from the trigonal structure is in the opposite sense to that found in rutile. Again the coordination around the metal atom is not a regular octahedron but contains four short and two long distances. The anionic lattice is less stable than in rutile even though it is a less dense structure, a consequence of the close O–O contact (2.46 Å) mentioned above. To complement our published results for rutile, we have performed tight-binding calculations on anatase too (using the parameters and geometric details described in the Appendix). The results of a bond overlap population analysis (**4**)

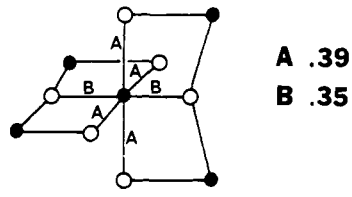

4

came from a calculation where all Ti–O distances were set equal. In contrast to rutile, these results are in accord not only with the sense of the observed bond lengths in the structure but also with that expected from the distortion at oxygen from **2** and **3**.

We have performed a series of computations on the anatase structure, similar to those described earlier[11] for rutile, to investigate the reasons behind the details of the observed structure. Figure 4 illustrates a variety of energetic trends as a function of the unique Ti–O–Ti angle in anatase. Clearly, neither a molecular orbital approach nor an electrostatic treatment alone can account for the observed geometry of anatase. O'Keeffe's approach, namely, maximizing the unit cell volume under constant Ti–O distances, predicts the Ti–O–Ti angle to be 141.1° (= $2(180° - \theta_{tet})$), much smaller than the observed angle of 156.3°. In quantitative terms the sum of the Coulombic repulsion between nearest-neighbor anion pairs and cation pairs shown in curve c of Figure 4 has a minimum at an angle less than 140°. However,

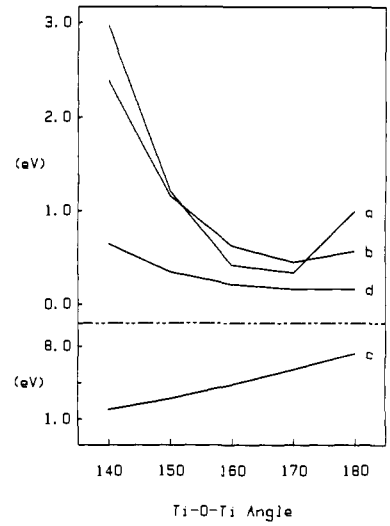

Figure 4. Energetics of distortion of TiO_2 in the anatase structure as a function of Ti–O–Ti angle. All Ti–O distances are fixed at 1.95 Å: (a) full tight-binding calculation on TiO_2; (b) tight-binding calculation for the oxide ions only from (a); (c) sum of nearest-neighbor Coulombic repulsions between O–O and Ti–Ti pairs—$E_c = \sum_i N_i/r_i$; (d) sum of nearest-neighbor pairwise interactions between oxygen atoms obtained from MO calculations on O–O dimers—$E_{(d)} = \sum_i V(r_i)$. The energy scale for all curves is electronvolts.

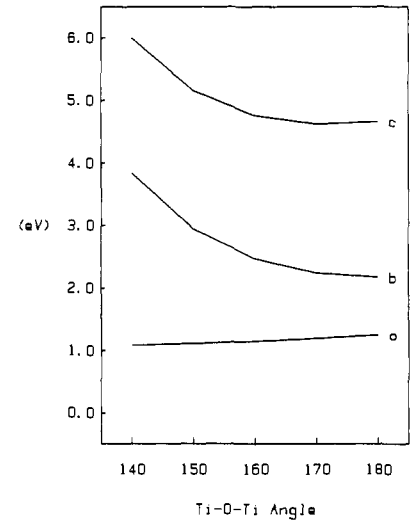

Figure 5. Energetic trends of the fragments found in anatase: (a) OTi_3^{10+} fragment; (b) TiO_6^{8-} fragment; (c) weighted average of (a) and (b). $E(c) = 2E(a) + E(b)$.

at such a Ti–O–Ti bond angle, there exists two short O–O contacts (the distance is 2.24 Å in the crystal) which are extremely influential in the molecular orbital approach. Curves a and b of Figure 4 show respectively energetics as a function of angle from tight-binding calculations on TiO_2 and the oxide lattice alone. This LCAO approach predicts the Ti–O–Ti angle to be ~166°, ten degrees larger than observed.

A major contributor to this result is the matrix effect of the oxide lattice, through the closed-shell repulsions of the O–O interactions across the shared edges of the octahedra. Curve d, which shows the variation in the sum of the nearest-neighbor pairwise interactions between oxygen atoms, emphasizes this effect. (Here we calculated the energy of an O_2^{4-} species as a function of distance.) The other major influence on the local geometry of oxygen is the local geometry at the metal. Figure 5 indicates the energetic trends with angle of the fragments OTi_3^{10+} and TiO_6^{8-} as well as their weighted sum: $2E(OTi_3^{10+}) + E(TiO_6^{8-})$. Besides the Ti–O bond distance distortions, the basal plane of the TiO_6 octahedron is not planar—the local point symmetry of the metal is $\bar{4}2m(D_{2d})$. Under such a distortion mode, both the Ti–O σ- and π-interactions are reduced, especially for large distortions.

However, the oxygen atom prefers a trigonal-planar environment, thereby competing with the tendency of the metal to remain ideally octahedral. The observed geometry of anatase arises from a compromise of forces tending to decrease the Ti–O–Ti angle—the matrix effect of the oxide network and the preference for trigonal-planar coordination of oxygen—with those promoting an increae in the Ti–O–Ti angle—the Coulombic/closed-shell repulsion between oxygen along the shared edges and the coordination preferences of the metal.

Let us see how the ideas of metal–oxygen π-bonding, described earlier make predictions concerning the relative Ti–O distances in these two structures. The local geometry around the metal atom in each arrangement is shown in **5** and **6** for rutile and anatase,

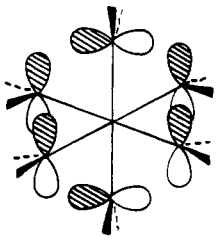

5

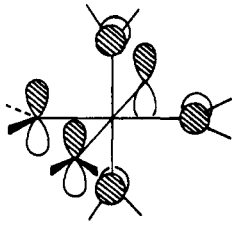

6

respectively. In rutile the two symmetry-inequivalent distances are associated with different π-overlap characteristics. Four of the linkages are associated with overlap of the oxygen p_z orbital with a single metal d orbital. Such interactions occur in pairs, one d orbital being involved in π-interactions with a trans pair of ligands. For the remaining two oxygen atoms overlap occurs with both of these. Here the oxygen p orbital bisects the Cartesian axes of the metal. To first order the overlap is the same as for the other oxygen orbitals. Such an analysis would suggest the presence of six Ti–O distances augmented by metal oxygen π-bonding of about the same length. In anatase the situation is different. Here too all of the oxygen p_z orbitals of the planar ligands can interact with the metal. However, the geometry is such that four of these ligand orbitals interact with just one central atomd d orbital, and the other two ligands interact each with a single metal d orbital. Sharing of a central atom orbital by more than one ligand decreases the individual π-strengths, the effect increasing with the number of ligands.[28] Such simple bonding ideas then tell us that there should be two short and four long metal–oxygen distances in anatase. However, in the observed structure there are two long and four short distances, a result that runs counter to this π-bonding argument. The ideas of π-bonding alone would suggest that the linkages in these species should be

$$\underset{\text{anatase}}{\text{four long}} > \underset{\text{rutile}}{\text{six short}} > \underset{\text{anatase}}{\text{two short}}$$

This is clearly *not* found in practice.

For the sake of comparison we show in Figure 6, the computed electronic densities of states for the two structures. Notice the broader "t_{2g}" part of the d band at around −9.5 eV for rutile, a result of the presence of straight chains, as distinct from the zigzag chains of anatase. As we have described elsewhere[11] by using the language of moments, the larger width of the rutile band is due to a larger fourth moment. Also notice the spike in the density of states at the top of the oxygen 2p region (at around −15 eV) of both systems, due to the p orbital which lies perpendicular to the OTi_3 plane and is involved in metal–oxygen π-bonding.

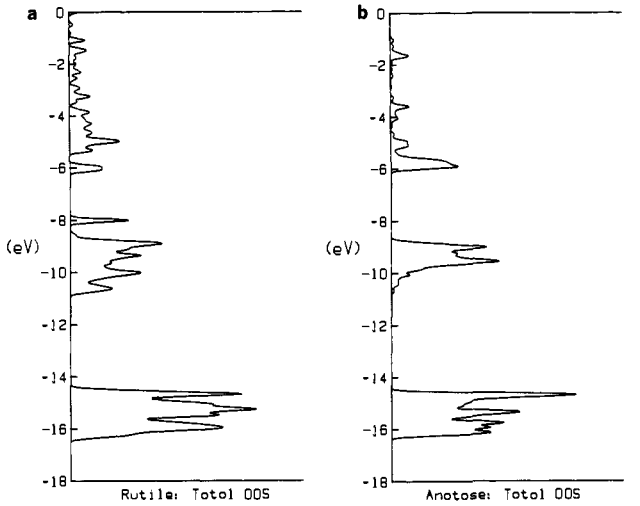

Figure 6. The electronic density of states of (a) the rutile and (b) the anatase polymorph of titanium dioxide. (The slight differences between the rutile plot and that of ref 5 are due to the use of a different smoothing width in the two computations.)

Table V. Details of the Coordination Polyhedron around Titanium and Predictions from Three Models

	anatase	rutile
	Ti–O Distances	
data		
obsd structure at 15 K	four short (1.9322 Å)	four short (1.9459 Å)
	two long (1.9788 Å)	two long (1.9764 Å)
	difference (0.0466 Å)	difference (0.0305 Å)
	average (1.9477 Å)	average (1.9561 Å)
temp change 293 → 15 K	−0.0016 (2) Å	−0.0027 (6) Å
	−0.0011 (9) Å	−0.0033 (8) Å
	Ti–O–Ti Angle	
unique angle at oxygen	156.3°	98.8°
predictions		
π-bonding model	two short	
	four long	six medium
bond overlap pop.	four short (0.39)	two short (0.44)
	two long (0.35)	four long (0.41)
O–O repulsns[a]	two long	two long
	four short	four short

[a] Using a model where the average Ti–O distance is fixed at the average value found in the real structure.

These results and observations are summarized in Table V. Notice that in addition to the comments concerning the individual pairs of distances, the shorter average distance in anatase is not commensurate with the relative values of the computed overlap populations for the two systems. The conclusion we draw from this discussion then is a rather interesting one. There seems to be no correlation of the details of the Ti–O linkages of the observed structures taken as a pair, with any of our electronic ideas, which in the past have often been useful in describing structural chemical problems. There is a similar problem with the calculations[29] recently reported by Post and Burnham using the MEG model. They obtained lowest energy structures geometrically close to those observed experimentally, but the distortion of the octahedron was in the opposite sense to that observed for rutile, while being correct for anatase. Their results then make the same predictions as those of our sets of overlap populations in **1** and **4**.

Molecular Mechanics Calculations

As we suggested in our earlier study,[11] the local geometrical details may then be set by the nature of the oxide–oxide interactions, which our rather crude orbital model does not mimic correctly. We have performed energy minimization calculations

(28) Burdett, J. K.; Albright, T. A. *Inorg. Chem.* **1979**, *18*, 2112.

(29) Post, J. E.; Burnham, C. W. *Am. Mineral.* **1986**, *71*, 142.

on the oxide ions alone of the rutile and anatase structures but this time with use of a Lennard–Jones 6–12 potential so arranged to give an energy minimum at 2.99 Å. (The details are given in the Appendix.) For both structures the energy is reduced by a distortion of the octahedron which is associated with a lengthening of one trans pair of Ti–O linkages (r_l) and a contraction of the other four (r_f), i.e., $r_l/r_f > 1$. (The metal atoms, of course, are not included in the calculation.) For rutile, energy minima were found for each value of u, the crystallographic parameter which fixes the oxide coordinates ($u = x_{oxygen} = y_{oxygen}$) as shown in **7**,

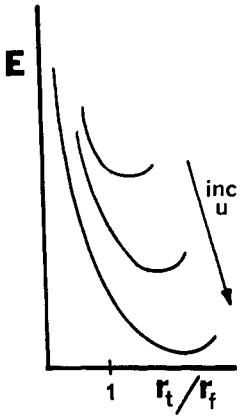

7

but both the magnitude of the distortion and the stabilization energy of the lattice increased as u increased. We were therefore unable to find a global minimum energy value for chemically sensible values of u, a direct result we believe of ignoring the Ti–O interactions in such a model. For anatase no minima in the energy were found for realistic values of u' (here equal to z_{oxygen}) or the ratio of axial to equatorial linkages, a result shown in **8**. The

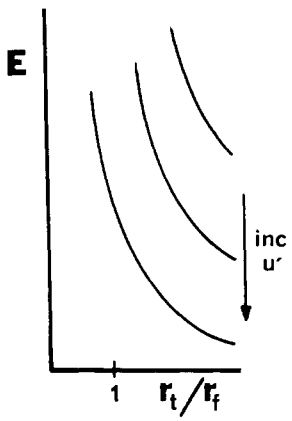

8

important conclusion however is that the oxide lattice *alone* will relax around the regular octahedral sites to give two long and four short M–O distances ($r_l/r_f > 1$) at these O–O separations rather than two short and four long ones.

For rutile we examined the energetic dependence of the curves on the average value of the Ti–O distance used in the calculation. As this distance increaes, so the energy curves of **7** become shallower in accord with qualitative ideas concerning such "ligand–ligand" interactions. As the metal–oxygen distance increases in these species, then we should expect to see a decrease in the importance of these interactions relative to the electronic ones we have described earlier. In fact for the series of rutile type oxides, the disparity between the bond lengths decreases[13] as the average metal–oxygen distance increases. For PbO_2 where the distances are equal within experimental error, the mean O–O contact is 3.08 Å. (The species CrO_2, RuO_2, and OsO_2 are exceptions to this rule, however. We will discuss them elsewhere.) The structures of rutile-type fluorides, however with longer metal–anion distances and smaller anions, have relative bond lengths in accord with a model where anion–cation interactions

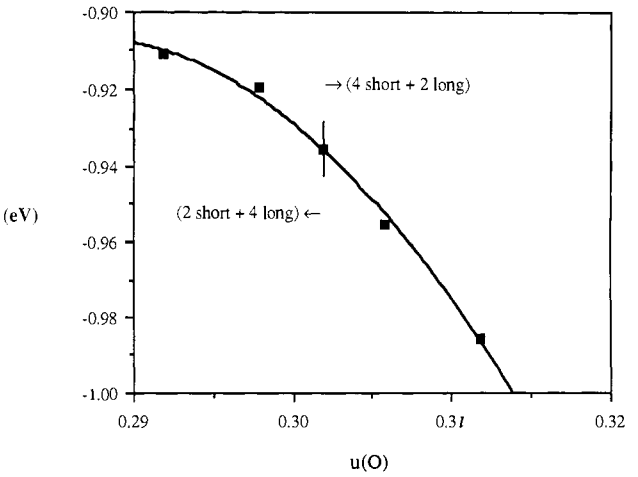

Figure 7. Total energy as a function of u(O) for the rutile structure of TiO_2 in which the lattice parameters a and c were fixed. The vertical line indicates the value of u(O) that produces equal Ti–O distances.

dominate the picture. Unless the systems are Jahn–Teller distorted the distortion away from octahedral is in accord with the results of **1**. (Hyde and O'Keeffe have recently shown how the sense of the distortion in these rutile-type oxides is indeed dependent upon the ratio of bonded to nonbonded distance.[30]) In this light we feel that the problem associated with the Post and Burnham study[29] is that the relative weight of the Ti–O and O–O potentials is incorrectly estimated. We note too the extremely poor agreement between observed and calculated rutile structures by Catlow and co-workers using a molecular mechanics approach.[31] In this study the O–O repulsive potential was of such short range that it was inconsequential. The overall result was then very little different from Pauling's many years ago.[32,33] A good agreement with the observed structures of rutile and anatase may be achieved by using this approach by judicious choice of attractive and repulsive potentials.[34] From this discussion, we would predict that for these "normal" fluoride species, if they could be made with the anatase arrangement, then the distortion of the octahedron should be in the opposite sense to that found in the known rutile analogue. This is simply because at these distances the dominant forces in controlling the asymmetry will be those directed between metal and fluorine and not between fluorine atoms.

Such a model is in accord with the unusual size of the thermal motion associated with the Ti atoms as determined experimentally. As we noted above, at room temperature the motion is as large for Ti as it is for O in rutile and a bit smaller for Ti in anatase. Such behavior is in accord with a titanium atom "rattling" in a hole in the structure whose size is determined by O–O repulsions. The smaller motion in anatase is in accord with the shorter mean Ti–O distance in anatase. In rutile-type fluorides where the coordination environment is controlled by direct cation–anion interactions, no unusual motion of the metal is found.

To complete our theoretical analysis of the rutile structure, we consider the distortion of the TiO_6 octahedron under the constraint of constant unit cell volume. In fact, we maintained constant lattice parameters and simply adjusted the u parameter for the oxygen positions. The total energy as a function of u(O) is shown in Figure 7, in which we mark the value of u(O) (0.302) that provides equal Ti–O distances for the two symmetry inequivalent bonds. These energetic trends match the structural observations—four short and two long Ti–O distances become preferred. Under the constaints imposed upon the unit cell, the only interactions that affect these energy changes are those involving Ti–O bonds and O–O repulsions. Since the distortion of

(30) Hyde, B. G.; O'Keeffe, M., unpublished results.
(31) Catlow, R. A.; James, R.; Mackrodt, W. C.; Steward, R. F. *Phys. Rev. B: Condens. Matter* **1982**, *25*, 1006.
(32) Pauling, L. *Z. Kristallogr.* **1928**, *67*, 377.
(33) The simplistic nature of the treatment in ref 31 is pointed out in: Mostoller, M.; Wang, J. C. *Phys. Rev. B.: Condens. Matter* **1985**, *32*, 6773.
(34) Smyth, J. R., unpublished results.

the local TiO_6 octahedron predicted from both the π-bonding arguments and the comparative overlap populations conflicts with observation, these computational results affirm the importance of O–O interactions in controlling the bond distances in TiO_2. Other local geometrical features, for example, the planarity of each OTi_3 unit, are also controlled by the π-interactions between Ti and O.

Our conclusions from this study are severalfold. There is not dramatic structural change concerning the metal coordination polyhedra as the temperature is lowered. The overall result is a small shrinkage in the metric of the lattice for both anatase and rutile. No large changes in bond lengths and angles are observed in contrast to those we have described for the open framework of cristobalite.[14] There is a small effect in anatase associated with the oxygen atom movement. Indeed in these close-packed structures these are the sorts of changes that should be expected. Only in more open structures should changes in the hinging of coordination polyhedra be found as the temperature is changed. However, the sense of the coordination geometry about the metal is the same at both temperatures and shows that the structure is clearly controlled by a balance of attractive Ti–O and repulsive O–O forces.

Acknowledgment. This research was supported by a generous grant to J.K.B. from the Dow Chemical Co. and by the National Science Foundation through Grant NSF DMR8276892 to the Materials Research Laboratory at The University of Chicago. J.W.R. acknowledges support of the Intense Pulsed Neutron Source By DoE, Contract W-31-109-ENG-38. This study is relevant to the attempt to understand the bonding of open-framework structures supporrted by Grant NSF CHE 84-05167. We also acknowledge J. D. Jorgensen of Argonne National Laboratory and J. J. Pluth and I. D. Steele for their experimental assistance.

Appendix

The tight-binding calculations were performed within the framework of the extended Hückel approach.[26] All Ti–O distances were set at 1.95 Å in both polymorphs. The geometry at oxygen was fixed by angles of 90°, 90°, and 135° in rutile and 155.8°, 102.1°, and 102.1° in anatase for the plots of Figure 4. The density of states curves were calculated by averaging over 40 special points in the irreducible wedge of the first Brillouin zone for the simple tetragonal lattice. Parameters for Ti and O were those used in the earlier study.[11] The plots of Figure 4a,b were obtained by variation of the u parameter of anatase while the Ti–O distance was kept fixed in an analogous way to the approach used in ref 11. The molecular mechanics calculations on anatase and rutile employed a finite cluster model consisting of nine unit cells of the crystal arranged in a tetragonal prism. The interaction energy of the four and eight oxide ions, respectively, in rutile and anatase, located in the central cell with the ions of all nine cells, was evaluated by using a simple Lennard–Jones potential with a minimum at 2.99 Å. With this requirement the shape of the curve is completely determined, but the energy units are arbitrary. We do not feel that trying to weight the energetic importance of the "electronic" and "hard sphere" effects is a useful exercise using our methods. The interaction energy was of sufficiently short range that this size prism was very adequate for this purpose. A two-dimensional energy surface in the coordinates u (which fixes the oxygen atoms positions in both structures) and the distortion coordinate q around the metal ion was constructed. If r_a, r_l, and r_f are respectively the average metal–oxygen distance and the distances of the symmetry-equivalent pair and quartet of distances in the real structure, then the distortion coordinate was that which kept the average metal–oxygen distance constant, i.e., $r_l = r_a + q$ and $r_f = r_a - (q/2)$.

Registry No. TiO_2, 13463-67-7.

Calcium-Selective Ligands. 2.[1] Structural and Spectroscopic Studies on Calcium and Cadmium Complexes of $EGTA^{4-}$

Cynthia K. Schauer and Oren P. Anderson*

Contribution from the Department of Chemistry, Colorado State University, Fort Collins, Colorado 80523. *Received August 1, 1986*

Abstract: The structures of salts of the calcium and cadmium complexes of the octadentate ligand $EGTA^{4-}$, Ca[Ca(EGTA)]·($^{22}/_3$)H_2O (**1**) and Sr[Cd(EGTA)]·7H_2O (**2**), have been investigated by single-crystal X-ray diffraction. **1** crystallizes in the monoclinic space group $P2_1/c$ (Z = 12), with a = 24.358 (4) Å, b = 16.798 (4) Å, c = 19.015 (4) Å, and β = 94.05 (2)°. **2** crystallizes in the monoclinic space group $P2_1/n$ (Z = 4), with a = 16.814 (4) Å, b = 8.454 (2) Å, c = 17.614 (5) Å, and β = 97.34 (2)°. Both Ca^{2+} and Cd^{2+} utilize the octadentate chelating capability of $EGTA^{4-}$ to form anions exhibiting distorted dodecahedral coordination spheres. In $[Ca(EGTA)]^{2-}$ anions, the nitrogen atoms bind to Ca^{2+} at longer distances (Ca–N(av) = 2.60 (2) Å) than do the ether oxygen atoms (Ca–O(ether, av) = 2.50 (3) Å) or the carboxylate oxygen atoms (Ca–O(carb, av) = 2.38 (2) Å). In $[Cd(EGTA)]^{2-}$, however, the nitrogen atoms bind to Cd^{2+} at shorter distances (Cd–N (av) = 2.43 (1) Å) than do the ether oxygen atoms (Cd–O(ether, av) = 2.580 (8) Å). The carboxylate oxygen atoms still bind at the shortest distances (Cd–O(carb, av) = 2.35 (5) Å). ^1H NMR spectra of the $[Ca(EGTA)]^{2-}$ and $[Cd(EGTA)]^{2-}$ anions show that in each case all carboxylate groups are made equivalent by intramolecular exchange at room temperature. The effect of dissociation of nitrogen ligand atoms, with subsequent inversion at nitrogen, is evident in ^1H NMR spectra for $[Ca(EGTA)]^{2-}$ at elevated temperatures. The ^{113}Cd chemical shift for $[Cd(EGTA)]^{2-}$ in solution (+15 ppm) reflects a more shielded environment for the ^{113}Cd nucleus than does the chemical shift (+36 ppm) for solid **2**. The ^{113}Cd powder pattern of **2** yields the three components of the shielding tensor (σ_{11} = +159, σ_{22} = +29, σ_{33} = −81 ppm); the most highly shielded component occurs in the range typical of cadmium-substituted calcium-binding proteins.

Structural aspects of the chelation of metal ions by highly polydentate ligands (i.e., ligands containing six or more binding sites) have recently become of interest in this laboratory. Many ligands in this category exhibit interesting patterns of metal-binding selectivity, yet, with the exception of $EDTA^{4-}$ (H_4EDTA = 3,6-bis(carboxymethyl)-3,6-diazaoctanedioic acid), little systematic structural knowledge exists regarding the manner in which such ligands bind to metals.

One important example of such selectivity is associated with the alkaline earth metal ions, Mg^{2+}–Ba^{2+}. In the body, mobile calcium (i.e., nonmineral calcium) is bound at a variety of sites

(1) Part 1: Schauer, C. K.; Anderson, O. P. *Acta Crystallogr., Sec. C: Cryst. Struct. Commun.* **1986**, *C42*, 760.

0002-7863/87/1509-3646$01.50/0